Tree Physiology Advance Access published March 17, 2015

Tree Physiology 00, 1–11
doi:10.1093/treephys/tpv020

Research paper

Slower phloem transport in gymnosperm trees can be attributed to higher sieve element resistance

Johannes Liesche[1,4], Carel Windt[2], Tomas Bohr[3], Alexander Schulz[1] and Kaare H. Jensen[3]

[1]Department of Plant and Environmental Sciences, University of Copenhagen, 1871 Frederiksberg, Denmark; [2]Forschungszentrum Jülich, IBG-2: Plant Sciences, 52428 Jülich, Germany; [3]Department of Physics, Technical University of Denmark, 2800 Kgs Lyngby, Denmark; [4]Corresponding author (joli@plen.ku.dk)

Received December 16, 2014; accepted February 10, 2015; handling Editor Maurizio Mencuccini

In trees, carbohydrates produced in photosynthesizing leaves are transported to roots and other sink organs over distances of up to 100 m inside a specialized transport tissue, the phloem. Angiosperm and gymnosperm trees have a fundamentally different phloem anatomy with respect to cell size, shape and connectivity. Whether these differences have an effect on the physiology of carbohydrate transport, however, is not clear. A meta-analysis of the experimental data on phloem transport speed in trees yielded average speeds of 56 cm h^{-1} for angiosperm trees and 22 cm h^{-1} for gymnosperm trees. Similar values resulted from theoretical modeling using a simple transport resistance model. Analysis of the model parameters clearly identified sieve element (SE) anatomy as the main factor for the significantly slower carbohydrate transport speed inside the phloem in gymnosperm compared with angiosperm trees. In order to investigate the influence of SE anatomy on the hydraulic resistance, anatomical data on SEs and sieve pores were collected by transmission electron microscopy analysis and from the literature for 18 tree species. Calculations showed that the hydraulic resistance is significantly higher in the gymnosperm than in angiosperm trees. The higher resistance is only partially offset by the considerably longer SEs of gymnosperms.

Keywords: carbon allocation, $^{14}CO_2$ labeling, isotope labeling, resistance model, sieve area, sieve plate, sieve pores, theoretical modeling, transmission electron microscopy.

Introduction

The phloem is the transport tissue of higher plants through which carbohydrates, the main unit for carbon transport, and other organic compounds are distributed between leaves and roots, fruits and other organs. Carbohydrate allocation in the phloem is a fundamental aspect of tree physiology with particular relevance for tree crop performance under changing climate conditions (Mildner et al. 2014). Knowing how fast carbohydrates are transported from leaves to roots in trees is a significant factor for the determination of carbon sequestration kinetics of forests and, therefore, for modeling the effects of climate change (Litton et al. 2007, Bonan 2008). However, functional data are scarce, since this transport pathway is experimentally inaccessible. Besides being buried below several tissue layers, the cells in question are under high pressure and thus, very sensitive to manipulation (Knoblauch and Peters 2010). This makes it a challenge to assess the influence of the diversity of phloem architecture on its function.

A meta-analysis of phloem transport measurements performed with the isotope-labeling technique indicated slower transport rates in conifers than in broadleaved trees (Epron et al. 2012). Such meta-analyses remain the only available tool to investigate principal differences between angiosperms and gymnosperms with regard to phloem transport, since no comparative studies involving more than three species have been done so far. In order to identify relevant parameters, meta-analysis of experimental data can be complemented by theoretical modeling. Theoretical models have been used to investigate the mechanism of carbon allocation and for the prediction of allocation patterns (Minchin and Lacointe

2005). Current models are simplified because many physical and physiological parameters remain unknown (De Schepper and Steppe 2010). Nevertheless, very simple transport resistance models were shown to predict phloem transport speed in several herbaceous plant species with good accuracy (Jensen et al. 2011).

Of the structural parameters in which angiosperms and gymnosperms differ, the sieve element (SE) architecture is especially likely to have a strong influence on phloem function. The SEs of gymnosperms are generally longer and thinner than in angiosperms. This principal difference in SE anatomy was already recognized by Hartig (1837), who compared SEs from conifer and woody dicots. He also described the structural differences of the axial cell connections of SEs, which were later shown in more detail with the help of transmission electron microscopy (TEM) analysis. The wide open sieve pores in the angiosperm sieve plate contrast with the plasmodesmata-like cell connections in the tapering end walls of gymnosperm SEs (Kollmann and Schumacher 1963, Evert and Alfieri 1965, Kollmann 1975, Schulz 1990).

The flow velocity of the phloem sap was found to be strongly influenced by the geometry of the conducting SEs in angiosperms (Thompson and Holbrook 2003, Mullendore et al. 2010). The anatomical differences led to speculation whether gymnosperms might use a different mechanism for whole-plant phloem transport in which functional units are relayed, instead of the single hydrostatic pressure gradient between source and sink in angiosperms (Schulz 1998). However, a recent study confirmed that the structural parameters of the transport system of gymnosperm trees follow the same scaling law as angiosperms, implying that they are optimized for phloem transport speed using the same Münch-type phloem transport mechanism (Jensen et al. 2012*a*). This raises the question whether the thinner SE and narrow sieve pores of gymnosperms have a physiological effect at all or if it is offset by longer SEs and higher sieve pore abundance.

Materials and methods

Meta-analysis of experimentally determined phloem transport speeds

Earlier compilations of results from tree phloem transport speed measurements by Liesche et al. (2013) and Mencuccini and Hölttä (2010) were used and supplemented with data from studies that report on phloem translocation in trees and explicitly state a value for transport speed. Some of these did not report the height of the sampled trees. In those cases tree age was used to estimate tree height with the help of values given on websites of foresters in the respective region.

Theoretical model of phloem transport speed

We obtained modeled phloem velocities from Jensen et al. (2012*a*). They computed the transport speed $v = Q/(\pi r^2)$ through conduits of radius r from calculations of the flow rate $Q = \Delta p/R_{tot}$ assuming a constant pressure differential $\Delta p = 0.7$ MPa (Turgeon 2010). When calculating the total resistance R_{tot}, Jensen et al. included the SE flow resistance (see Eq. (1)), and the resistance to flow of water across cell membranes in parts of the plant where loading and unloading of photoassimilates occurs $R_{tot} = (H/L)R_{SE} + 1/(2\pi rmL_p)$. The parameter L_p is the permeability of the cell membrane, H is the transport distance, L is the length of one SE, R_{SE} is the SE resistance and m is the leaf lamina length. Note that the pre-factor H/L corresponds to the number of SEs lying end-to-end along the transport pathway, and that the pressure difference Δp is therefore over the transport distance H. The following values were used for the variables viscosity $\eta = 2$ mPa s, pressure differential $\Delta p = 0.7$ MPa and cell membrane permeability $L_p = 5 \times 10^{-12}$ m s^{-1} Pa^{-1}.

Meta-analysis of SE data

Data were collected from literature sources that stated values of SE length, SE diameter, number of sieve areas per end wall, number of pores per sieve area, pore diameter and pore length. In most cases, complete data sets were obtained by combining parameters from different sources.

TEM of sieve areas

Sample collection, specimen preparation and TEM imaging were performed as described by Schulz and Behnke (1987). Stem samples from *Fagus sylvatica* L., *Picea abies* (L.) Karst and *Abies alba* Mill. L. were collected in the Schwarzwald (47°48′24.7″N, 7°46′07.3″E) and Odenwald (49°26′N, 8°49′E) regions in Southwest Germany during the vegetation period. *Picea abies* and *A. alba* trees were ~70 years of age, while *F. sylvatica* trees were ~120 years old. Stem samples were cut at breast height (1.3 m) as narrow rectangles (20 × 5 × 2 mm), as deep as the cambium, and transferred to primary fixative solution, paraformaldehyde–glutaraldehyde solution in 0.1 M cacoldylate buffer. After primary fixation for 3–12 h, samples were washed several times with Na-cacodylate buffer (pH 7.3) and secondarily fixed for 1 h with 1% osmium tetroxide. Following washing and acetone dehydration series, samples were embedded in Epon–Araldit resin and polymerized for 36 h at 60 °C. Semi-thin sections stained with crystal violet were used for identification of areas of interest. Ultra-thin sections were stained with uranlylacetate and led citrate before analysis in a Phillips EM400 electron microscope. From the more than 1000 images of originally 42 samples, 80 images of one tree per species were selected that had adequate clarity and resolution for the determination of the parameters in question.

Theoretical modeling of sieve area resistance

We modeled the resistance of a single SE R_{SE} as the sum of two components: the lumen resistance R_L and the end-wall resistance R_{EW}

$$R_{SE} = R_L + R_{EW}. \quad (1)$$

We approximated the lumen resistance $R_L = 8\eta L/(\pi r^4)$ by the Hagen–Poiseuille factor relating flow rate Q to pressure differential Δp across a cylindrical tube. Here, the factor L is the length of the SE while r is the radius and η is the viscosity of the phloem sap. To estimate the end-wall resistance R_{EW} we assumed that the sieve pores can be modeled as a collection of short cylindrical pipes running in parallel. The end-wall resistance thus depended on the thickness of the sieve plate l, the pore radius r_p and the number of pores. For the simplest case of N identical pores, the end-wall resistance is

$$R_{EW} = \frac{1}{N}\left(\frac{3\eta}{r_p^3} + \frac{8\eta l}{\pi r_p^4}\right). \quad (2)$$

The first term in the bracket is due to viscous friction at the pore entrance and the second term is the Hagen–Poiseuille factor. Jensen et al. (2012*b*) pointed out that Eq. (2) is sensitive to small variations in the pore radius r_p, which typically varies by up to 25% between different conduits. To account for the added flow through a few large pores, we follow Jensen et al. (2014) and write

$$R_{EW} = \frac{1}{N}\left(\frac{3\eta}{r_p^3} A + \frac{8\eta l}{\pi r_p^4} B\right). \quad (3)$$

Here, r_p denotes the average sieve pore radius and the parameters $A = 1/(1 + 3(\sigma/r_p)^2)$ and $B = 1/(1 + 6(\sigma/r_p)^2 + 6(\sigma/r_p)^4)$, where σ is the standard deviation of the sieve pore radii. Typical values are around $\sigma/r_p \simeq 1/2$ corresponding to $A \simeq B \simeq 1/2$.

Results

The meta-analysis of experimental data and a simple resistance model indicate a principally lower phloem transport speed in gymnosperm compared with angiosperm trees

Phloem translocation speeds in trees have been measured by a wide range of experimental methods (Millburn and Kallarackal 1989, Epron et al. 2012). In Table 1 all translocation speed measurements performed on trees that we are aware of are compiled, including details on the methods that were used to measure them.

Integrating the data of all experiments, an average phloem transport speed of 56.3 cm h^{-1} for the 20 measurements on angiosperm trees is found, a value that is significantly higher than the average value of 21.9 cm h^{-1} that was found for 26 gymnosperms (Figure 1a). No clear correlation can be seen when looking at the relationship between phloem transport speed and tree height, the only relevant parameter that is available for all studies (Figure 1b).

In order to identify the parameter(s) that could cause the difference in transport speed between the two genera, we utilized a simple resistor model that was shown to successfully predict phloem transport speed in herbaceous plants (Jensen et al. 2011). The anatomical data necessary for this model were obtained from Jensen et al. (2012*a*). The data set contains parameters for 31 gymnosperm and 16 angiosperm tree species (Table S1 available as Supplementary Data at *Tree Physiology* Online). Of the trees that experimental phloem speed measurements were performed on, one-third are represented in the data set used for theoretical modeling. On a family level, two-thirds are represented in both data sets.

The calculated average phloem translocation speeds for angiosperm and gymnosperm trees are 49.9 and 29.4 cm h^{-1}, respectively (Figure 1c). The modeled difference is slightly smaller than in the experimental data (Figure 1a), but is still significant. In order to investigate which model parameter(s) caused the difference in phloem transport speed predictions, the average values for relevant model parameters were plotted. While there was no difference in average stem length between the two groups (Figure 1d), the average effective SE radius of angiosperm trees was found to be significantly higher than in gymnosperm trees (Figure 1e). This indicates that the SE architecture has a strong influence on overall transport speed.

Quantitative sieve area anatomy of Fagus sylvatica, Abies alba and Picea abies

So far, the lack of quantitative data on the architecture of gymnosperm SEs, and especially regarding the number and size of sieve pores, has prevented a comparative analysis of flow resistance. The structure of sieve plates in the phloem of various angiosperms was recently determined with the help of scanning electron microscopy after clearing the cells of cytosolic content (Mullendore et al. 2010). These data were subsequently used to describe the hydrodynamic properties of angiosperm sieve plates with the help of theoretical modeling (Jensen et al. 2012*b*). Corresponding data for gymnosperms are not available.

Here, parameters necessary for modeling of gymnosperm phloem hydraulics, SE length, SE diameter, number of pores in the end-wall, pore diameter and pore length were extracted from literature sources (Table 2). These combined data sets were complemented by our own measurements using TEM. Images were obtained from a single tree of, respectively, the angiosperm *F. sylvatica*, and the gymnosperms *A. alba* and *P. abies*.

The images show the clear difference in SE end-wall structure (Figure 2) that is also apparent in the literature data (Table 2). Like most, but not all angiosperms, *F. sylvatica* SEs have one sieve area per sieve plate with the typical wide open pores (Figure 2a). *Picea abies* and *A. alba* SEs feature numerous sieve areas in their long overlapping end walls (Figure 2b) as found in all gymnosperm species (Table 2). Pore length and diameter of the gymnosperm species could be measured on high magnification tangential sections (Figure 2c), while the number of pores per

Table 1. Experimentally determined phloem translocation speeds in trees. VPD, vapor pressure deficit; T, temperature.

Species	Transport speed (cm h^{-1})	Stem length (m)	Method	References
Gymnosperms				
Picea sitchensis	2.7	4[1]	Tracking ^{14}C pulse along stem	Watson (1980)
Picea mariana	4.1	4	Tracking ^{14}C pulse between branch and roots	Carbone et al. (2007)
Abies concolor	5.5	20[1]	Tracking ^{14}C pulse along branch	Leonard and Hull (1965)
Abies procera	5.7	2[1]	Tracking ^{14}C pulse along stem	Watson (1980)
Pseudotsuga menziesii	7.4	8	Correlation of VPD and ecosystem $\delta^{13}C$	Bowling et al. (2002)
Pinus banksiana	9	0.8[1]	Tracking ^{11}C pulse along stem segments	Thompson et al. (1979)
Pinus sylvestris	10	2.4	Tracking ^{13}C pulse between needle and stem base	Högberg et al. (2008)
Picea mariana	11	0.7[1]	Tracking ^{11}C pulse along stem	Thompson et al. (1979)
Abies nordmanniana	11.5	0.5	Tracking ^{14}C pulse along stem	Liesche (unpublished)
Abies nordmanniana	14	0.3	Tracking ^{14}C pulse along stem	Liesche (unpublished)
Pinus taeda	15	7.2	Tracking ^{13}C pulse between canopy and stem base phloem	Warren et al. (2012)
Larix decidua	15	1.2[1]	Tracking ^{14}C pulse along stem	Schneider and Schmitz (1989)
Pinus pinaster	16	9	Tracking ^{13}C pulse along stem	Dannoura et al. (2011)
Juniperus occidentalis	16.6	10	Correlation of VPD and ecosystem $\delta^{13}C$	Bowling et al. (2002)
Picea abies	18.3	22	Correlation of VPD and T with soil efflux $\delta^{13}C$	Ekblad et al. (2005)
Picea abies	18.3	17.2	Correlation of VPD and T with soil efflux $\delta^{13}C$	Comstedt (2008)
Pinus taeda	20.5	17.2	Correlation of VPD with soil efflux $\delta^{13}C$	Mortazavi et al. (2005)
Pseudotsuga menziesii	21.3	23	Correlation of VPD with ecosystem $\delta^{13}C$	Bowling et al. (2002)
Pseudotsuga menziesii	23.3	28	Correlation of canopy conductance with ecosystem $\delta^{13}C$	Pypker et al. (2008)
Pinus sylvestris	26.7	2	MRI velocimetry in stem	Windt (unpublished)
Pinus ponderosa	27.5	33	Correlation of VPD with ecosystem $\delta^{13}C$	Bowling et al. (2002)
Pinus sylvestris	31.3	22.5	Correlation of RH with soil efflux $\delta^{13}C$	Ekblad and Högberg (2001)
Pinus ponderosa	45.8	22	Correlation of VPD and PAR with soil efflux $\delta^{13}C$	McDowell et al. (2004)
Metasequoia glyptostoboides	58	25[1]	Tracking of ^{14}C pulse along branch	Willenbrink and Kollmann (1966)
Pinus sylvestris	60.4	14.5	Correlation of VPD and T with phloem $\delta^{13}C$ at stem base	Brandes et al. (2006)
Pinus sylvestris	75	15	Tracking $\delta^{18}O$ along stem	Barnard et al. (2007)
Angiosperms				
Fagus sylvatica	24.5	2.5	MRI velocimetry in stem	Windt (unpublished)
Nothofagus solandri	25	18	Correlation of ecosystem $\delta^{13}C$ with phloem $\delta^{13}C$	Barbour et al. (2005)
Populus sp.	26.5	0.5[1]	Tracking of ^{32}P pulse along stem	Vogl (1964)
Nothofagus solandri	27.8	20	Correlation of ecosystem $\delta^{13}C$ with phloem $\delta^{13}C$	Barbour et al. (2005)
Salix sp.	29	0.8[1]	Tracking of ^{14}C pulse inside phloem along stem	Peel and Weatherley (1962)
Fagus sylvatica	40	0.8	Tracking of ^{13}C pulse between canopy and soil respiration	Barthel et al. (2011)
Fraxinus excelsior	41.6	0.7[1]	Tracking of ^{11}C pulse along stem	Jahnke et al. (1998)
Ulnus americana	42.9	0.9[1]	Tracking of ^{11}C pulse along stem	Thompson et al. (1979)
Populus nigra	43	0.35	Tracking of ^{11}C pulse along stem	Babst et al. (2005)
Fagus sylvatica	43	26	Correlation of VPD and stomatal conductance with phloem $\delta^{13}C$ at stem base	Keitel et al. (2003)
Sorbus aucuparia	44.65	0.7[1]	Tracking of ^{11}C pulse along stem	Jahnke et al. (1998)
Fraxinus americana	48	0.9[1]	Tracking of ^{11}C pulse along stem	Thompson et al. (1979)
Fraxinus americana	50	15[1]	Change in concentration ratio of different sugars in the phloem sap at different positions along the stem	Zimmermann (1969)
Croton macrostachyus	60	5.1	Tracking of ^{13}C pulse between canopy and phloem at stem base	Shibistova et al. (2012)
Quercus petraea	69	9	Tracking of ^{13}C pulse along stem	Dannoura et al. (2011)
Fagus sylvatica	71.5	9	Tracking of ^{13}C pulse along stem	Dannoura et al. (2011)
Salix viminales	100	0.7[1]	Flow speed is inferred from stylet exudation rate in the stem	Weatherley et al. (1959)
Fagus sylvatica	100	10	Tracking of ^{13}C pulse between canopy and stem respiration	Plain et al. (2009)
Podocarpus falcatus	117.5	6.2	Tracking of ^{13}C pulse between canopy and phloem at stem base	Shibistova et al. (2012)
Populus tremula x alba	122.4	0.4	MRI velocimetry in stem	Windt et al. (2006)

[1]Estimate.

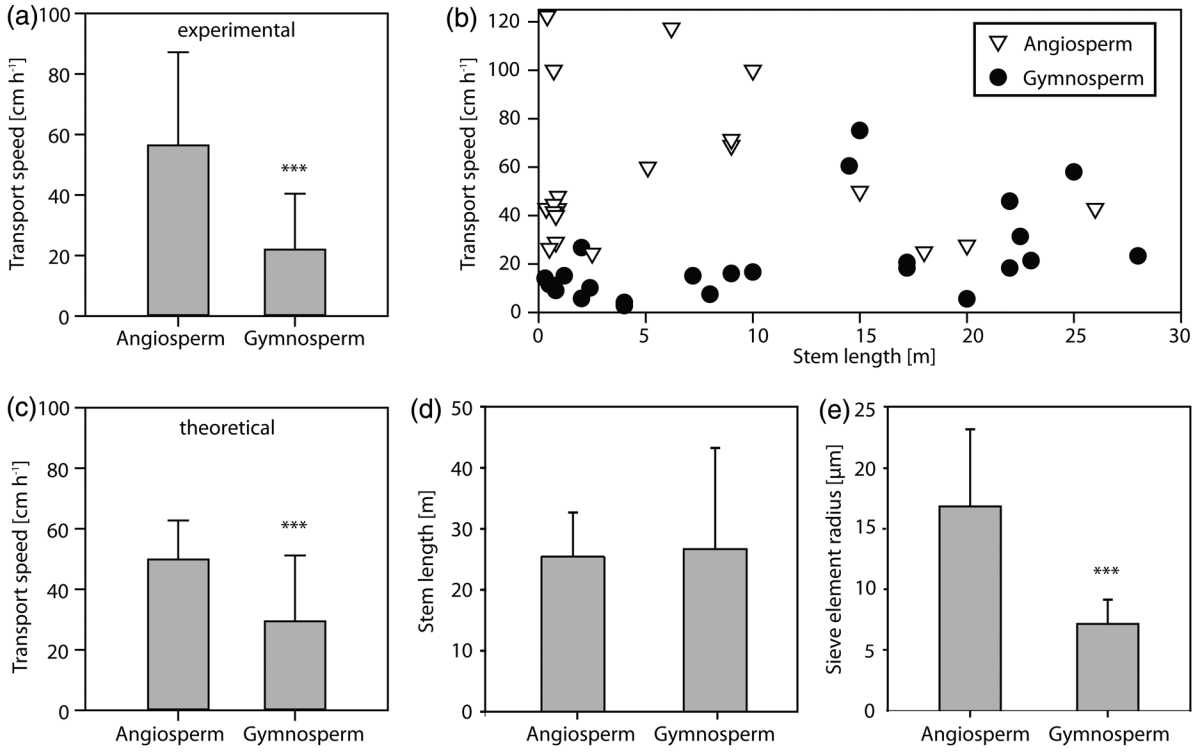

Figure 1. Comparison of phloem transport speeds in angiosperm and gymnosperm trees. (a) Average transport speed for 26 gymnosperm and 20 angiosperm trees from experiments reported in the literature. (b) Experimentally determined phloem transport speeds as a function of tree height. (c) Average transport speed for 31 gymnosperms and 16 angiosperm trees predicted using theoretical modeling. (d) Average stem length of the trees used for the theoretical modeling approach. (e) Average effective sieve element radius of the trees used in the theoretical approach. Asterisks indicate statistical significance with $P < 0.001$.

sieve area could be determined with the help of glancing sections (Figure 2d).

Calculation of sieve area resistance in angiosperm and gymnosperm trees

Using numerical simulations, Jensen et al. (2012*b*) found mathematical expressions for the resistances to flow across sieve areas and inside SEs. Applying the equations to the data obtained from literature and by TEM analysis (Table 2), the relationship between lumen and SE end-wall resistance can be calculated and the SE resistance directly compared between gymnosperm and angiosperm trees.

The analysis shows a clear difference in overall SE resistance between angiosperm and gymnosperm trees. The average end-wall resistance of gymnosperm trees is ~70 times higher than for angiosperm trees (Figure 3a). Even when taking into account that fewer end walls are present in gymnosperm phloem because of the longer SEs, by calculating resistance per unit length, there is a difference of about factor of 10 (Figure 3b). Our own data, in which all parameters for each species were measured on a single tree, are in agreement with the literature data, which comprises information from several trees per species (numbers 3, 13, 16 in Figure 3).

Furthermore, the analysis indicates a ratio between lumen resistance and end-wall resistance that is close to 1 : 1 in all trees (Figure 3a). This ratio was observed in all angiosperms that have been investigated so far (Jensen et al. 2012*b*).

Discussion

Phloem transport is slower in gymnosperm trees than that in angiosperm trees

Both theoretical modeling based on anatomical data and the summation of all experimental measurements found in the literature suggest that gymnosperm trees exhibit slower phloem transport speed than angiosperm trees. Theoretical as well as experimental methods to measure or predict phloem transport speeds in trees are prone to a wide variety of errors. In the case of the theoretical model, only a subset of the relevant parameters was taken into consideration, which were phloem loading strength, pathway length and anatomy, phloem sap viscosity and the pressure differential. In particular the pressure differential, which so far has not been conclusively determined in trees (Turgeon 2010), could significantly change the results. The differential of 0.7 MPa is mostly based on measurements on angiosperm trees and a principal difference in relation to gymnosperm trees cannot be excluded. Sieve element dimensions

Table 2. Anatomy of sieve elements and sieve areas. All values in μm.

No. in Fig. 3	Species	Sieve element length	Sieve element diameter	Number of sieve areas per end wall	Number of pores per sieve area	Pore diameter	Pore length (end-wall thickness)	References
Angiosperms								
1	*Ailanthus glandulosa*	180	48	1	50	2.5	0.6	MacDaniels (1918)
2	*Antiaris africana*	305	31	1	29	7	1	Lawton (1972)
3	*Fagus sylvatica*	195 ± 52	24.23 ± 6.568	1 ± 0	45 ± 10	2.925 ± 0.8561	1.186 ± 0.252	This study
4	*Holarrhena floribunda*	275	25	4.5	69	0.9	0.8	Lawton (1972)
5	*Populus deltoides* Marsh.	165	39.00	11.5	25	4.75	0.9	MacDaniels (1918), Larson and Isebrands (1974)
6	*Prunus persica*	243.00	33.00	1	130	1.5	1	Donghua and Xinzeng (1993), Moing and Carde (1988)
7	*Pyrus malus*	250	22	6	52	1.2	1	MacDaniels (1918), Esau and Cheadle (1958)
8	*Robinia pseudoacacia*	180	20	1	21	2.5	0.5	Tyree et al. (1974)
9	*Sabal palmetto*	700	36	1	287	1.9	0.5	Parthasarathy and Tomlinson (1967)
10	*Tectona grandis*	300	35	1	96	2.5	0.7	Lawton (1972)
11	*Tilia americana*	350	30	1	625	1.2	0.8	Tyree et al. (1974), Evert and Murmanis (1965)
12	*Ulmus americana*	190	36	1	50	4	1	Sheehy et al. (1995), Evert and Deshpande (1969)
Gymnosperms								
13	*Abies alba*	2500 ± 600	14.26 ± 2.938	18.75 ± 4.234	27 ± 4.1	0.372 ± 0.0796	1.95 ± 0.160	This study
14	*Cycas revoluta*	1350	13	19	12	0.5	1.3	Behnke (1986, 1990)
15	*Gnetum gnemon*	850	16	14	12 ± 3	0.61	1.6	Behnke and Paliwal (1973), Behnke (1990)
16	*Picea abies*	3300 ± 700	18.28 ± 3.10	25 ± 5	32 ± 4.2	0.335 ± 0.08	1.11 ± 0.181	This study
17	*Pinus pinea*	2800	22	21	20 ± 2.5	0.41	2.2	Chang (1954), Wooding (1966)
18	*Pinus strobus*	1580	21.8	28	25 ± 4	0.35	2.5	Crafts and Crisp (1971), Murmanis and Evert (1966), Evert and Alfieri (1965)

vary widely within a plant and in trees, the average SE radius was shown to slightly increase towards the stem base (Petit and Crivellaro 2013). A different scaling factor of SE radius with tree height in angiosperm and gymnosperm trees would lead to deviation of the modeled results. However, the limited available data suggest similar scaling for both groups (Petit and Crivellaro 2013). Other parameters are expected to scale in a similar way for both angiosperms and gymnosperms. One major parameter that was not considered in the resistor model and that could be expected to be different between the two taxa is the SE end-wall resistance. This means that predictions of phloem transport speed for gymnosperms would be even lower relative to that in angiosperms if the data presented here were to be taken into consideration.

A direct comparison of experimental phloem transport data derived from different studies is generally problematic because of the differences in the methodologies that were used, as well as differences in plant age, height and the environmental factors under which they were grown (Dannoura et al. 2011). Also the environmental factors under which measurements are performed can influence the results. A detailed discussion of methodologies and how they could lead to differences in the measured transport speed is presented by Mencuccini and Hölttä (2010).

Of the many different parameters that may influence the phloem transport velocity measurements, only information on methodology and tree height is reported for all experiments in the literature (Table 1). Several techniques have been employed, but, important in this context, most techniques have been used on both gymnosperms and on angiosperms, minimizing the potential for measurement bias. Exceptions are the tracking of $\Delta^{18}O$ along the stem, which has only been used on *Pinus*

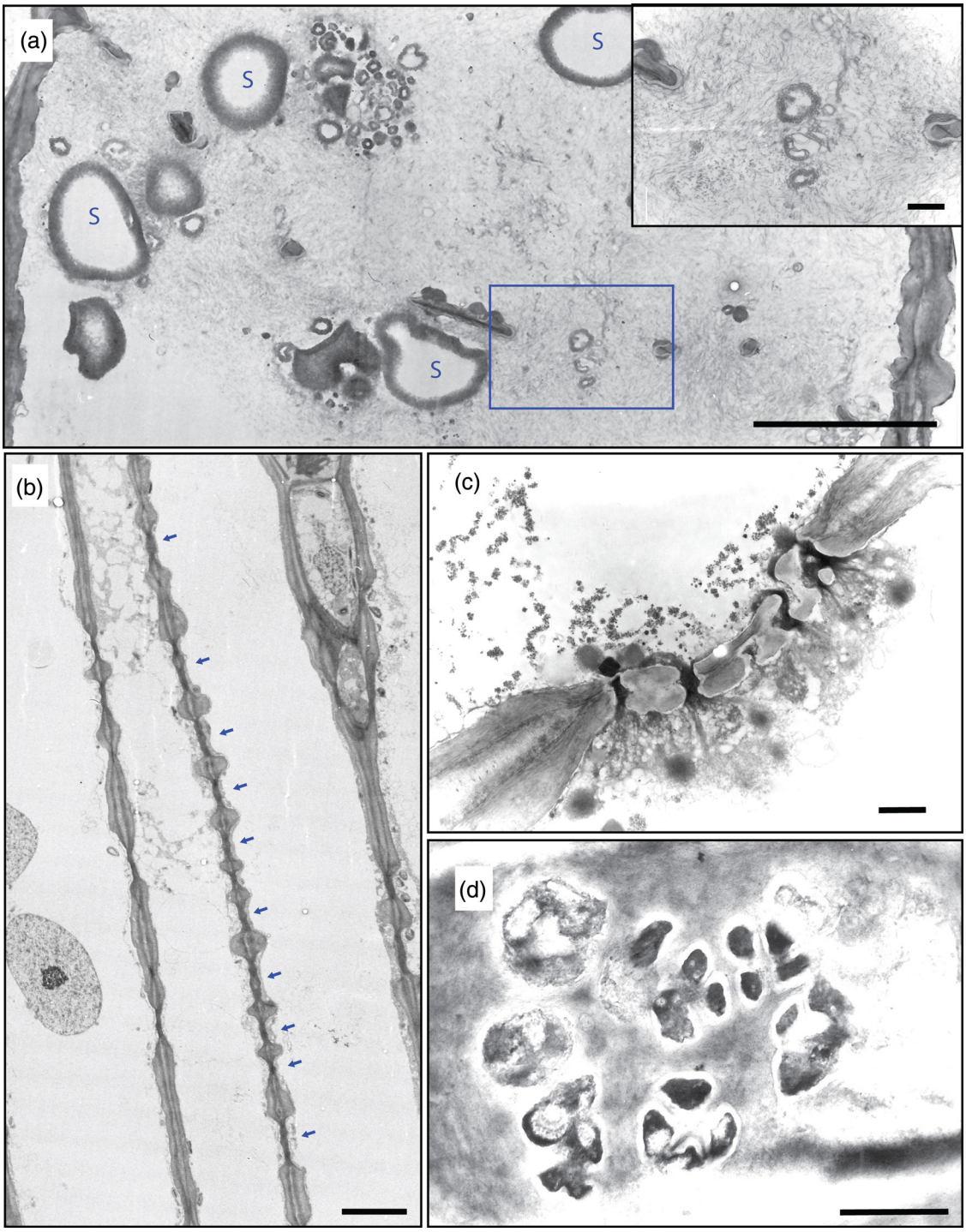

Figure 2. Sieve area anatomy of angiosperm and gymnosperm trees. (a) Lateral section through stem phloem of the angiosperm *F. sylvatica* showing the connection of sieve elements by wide open pores. The starch-storing sieve element plastids are marked by 'S'. The inset shows a magnified view of one sieve pore. (b) Lateral section through stem phloem of the gymnosperm *A. alba* showing numerous sieve areas (arrows) along the wall between overlapping sieve elements. Cross section (c) and glancing section (d) of single *A. alba* sieve area. The white area around the sieve pores corresponds to the callose collar. Black structures inside the pores correspond to electron-dense material that stems from the preparation. Scale bars (a and b) 10 µm, inset in (a, c, and d) 1 µm.

sylvestris (Barnard et al. 2007), and the analysis of the sugar composition of the phloem along the stem, which was used on *Fraxinus americana* (Zimmermann 1969). In the case of *P. sylvestris*, the measured speed is the highest for any gymnosperm and considerably higher than measurements on trees of the same species conducted by different methods (Table 1), indicating that the method may be biased towards higher speeds. In the case of *F. americana*, the measured value

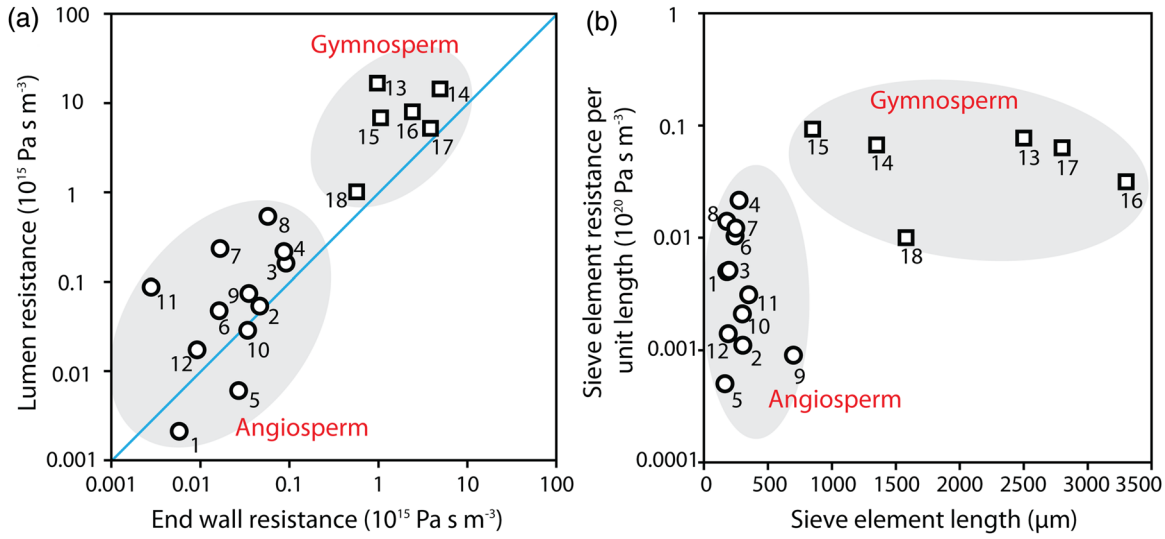

Figure 3. Sieve element resistance. (a) Angiosperm trees (circles) and gymnosperm trees (squares) show the same 1 : 1 ratio (line) between lumen and sieve area resistance. (b) Sieve element resistance corrected for sieve element length.

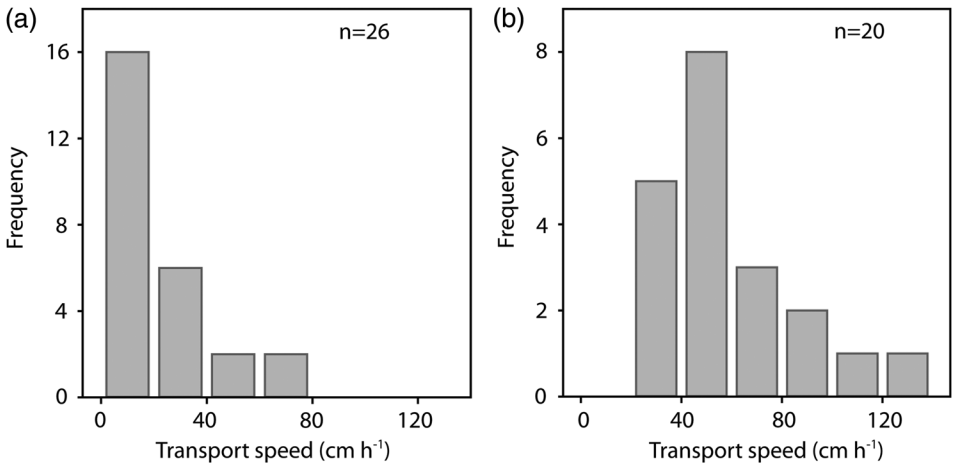

Figure 4. Histograms of phloem transport speed data from gymnosperm (a) and angiosperm (b) trees. Data from Table 1.

is close to the angiosperm tree average and to measurements made on trees of the same species with other methods, suggesting that the measurement was accurate.

The average tree height of the sampled trees is ~12 m for gymnosperms and ~7 m for angiosperms. It has been suggested that phloem hydraulic conductance scales with tree height (Hölttä et al. 2013). The only study that addresses the question of whether phloem transport speed scales with tree height found a correlation between height and transport speed in *F. sylvatica* but not in *Quercus* and *Pinus* (Dannoura et al. 2011). Moreover, there is no indication for a particular correlation in the data presented here.

The present paper suggests that angiosperms achieve higher transport speeds than gymnosperms. This is supported by measurements that, using the same method, directly compare transport speeds of gymnosperm and angiosperm trees. The studies that involve both gymnosperm and angiosperm trees, including data from MRI velocimetry and carbon-tracer experiments, clearly show a lower phloem translocation speed in gymnosperms compared with angiosperms (Thompson et al. 1979, Dannoura et al. 2011). The high number of species from which data were taken into account and the robustness of this trend in both the theoretical and experimental approach suggests that the result reflects a true physiological difference between angiosperm and gymnosperm trees.

Higher SE and end-wall resistance in gymnosperm trees

The quantification of structural parameters of the phloem translocation system in gymnosperms has been a significant challenge. In particular the number and size of sieve pores that connect SEs axially were difficult to determine, since their small size prevents accurate resolution with light microscopy. In addition, their diameter is not constant along their length. While TEM was used to provide qualitative information on the pore structure

(Kollmann and Schumacher 1963, Murmanis and Evert 1966, Behnke and Paliwal 1973), in most cases, only a low number of pores per sieve area were analyzed. Furthermore, no complete data sets from the same tree were available that contain all necessary data to determine flow resistance in gymnosperms.

Here, TEM was used to provide these data for two gymnosperms and one angiosperm. We were forced to limit ourselves to three tree species due to the enormous effort that is necessary to obtain enough image material to determine all parameters reliably. Errors could be introduced due to intra-species variation of SE and end-wall structure, although parameters of the analyzed trees were cross-referenced with data from other trees in the same forest stand. The presence of a higher end-wall resistance in gymnosperms is further supported by data in the literature (Table 2).

Interestingly, when the lower number of end walls in gymnosperms is taken into account, the total SE resistance still seems to be an order of magnitude higher in gymnosperm trees than in angiosperms. This is true for the species for which data for single trees were provided and is generally supported by the metadata collected from various literature sources as well (Table 1). There could be two reasons why this difference in resistance per unit length does not lead to an equally high difference in phloem transport speed. First, considering the histograms of the transport speed data (Figure 4), it becomes apparent that the gymnosperm distribution (Figure 4a) is heavily skewed toward lower speeds (resembling an exponential distribution). The angiosperm distribution, in contrast, approximates a Weibull curve with shape parameter ~2. Even though the average speed differs by a factor of 2, the medians of the two distributions differ by a factor of 3. Second, gymnosperms tend to have shorter leaves than angiosperms of comparable height (see Figure 2a in Jensen et al. 2012*a*), a fact that according to the equation for the total resistance (Eq. (1)) further reduces the speed. It should be noted that non-permanent structures inside the SEs, specifically P-Protein, callose or ER membranes, were not considered when determining parameters like sieve pore size. This adds some uncertainty to the values that we obtained for both the angiosperm and gymnosperm trees. It could, however, be argued that if we make an error in this fashion, it would result in an under-estimation of gymnosperm SE resistance instead of an over-estimation, because the presence of ER accumulations on end walls has been demonstrated in vivo (Schulz 1992).

Regarding the ratio of lumen and end-wall resistance, it was observed that the value for all trees is very close to 1 : 1, although slightly shifted to higher lumen resistance. This could be due to the fact that the presence of callose, which can be expected to form a slim collar around sieve pores even in the intact state, was not considered in the calculation of end-wall resistance. The observations would then match earlier studies for angiosperms, lending support to the hypothesized existence of a general allometric scaling law for end-wall resistance (Jensen et al. 2012*b*). The one-to-one relationship between lumen and end-wall resistance is not unique to the phloem; similar trends have been observed in the link between xylem lumen and end-wall resistance as well (Wheeler et al. 2005). The correspondence may be explained by the diminishing return in terms of added mass flow when either resistance component is reduced (Charnov 1976).

Is SE resistance causing slower phloem transport speeds in gymnosperm trees?

In addition to the difference in SE resistance, there are several factors that could cause phloem transport to be slower in gymnosperm trees than in angiosperm trees. Evaluating the influence of different factors on the transport speed difference is far easier for the data based on theoretical modeling since it is based on relatively few parameters. The lower phloem translocation speeds that were observed in gymnosperms were not due to lower tree heights, which were the same on average. Furthermore, our data suggest that speed does not scale with tree height. While leaf length, which is used as a parameter for source strength in the model, is on average ~60% lower for gymnosperms, its impact on phloem transport speed predictions is limited. Instead, the SE radius is the decisive model parameter that results in the difference in phloem transport speeds. After correcting for the differences in SE shape, which has an effect on the hydraulic conductance, the effective radius is, on average, 58% smaller in gymnosperms than in angiosperm trees. The effective SE radius does not scale with tree height, but instead remains in a range of 4–12 μm for gymnosperms and 5–25 μm for angiosperm trees (Jensen et al. 2012*a*). Since our results show that sieve plate and lumen contribute almost equally to the total hydraulic resistance of the phloem translocation pathway, the predictions based on effective SE radius, even when sieve plates are not considered in the model, will be qualitatively correct.

To identify the decisive factor(s) that determines transport speed differences in experimental measurements is difficult due to the high number of variables that affect such measurements. Nevertheless, many factors are normalized across the data range considered here, leaving SE resistance as the only factor for which a principal difference between angiosperm and gymnosperm trees could be clearly shown.

Supplementary data

Supplementary data for this article are available at *Tree Physiology* Online.

Conflict of interest

None declared.

Funding

This study was supported by funding from the Danish Council for Independent Research provided to A.S. and T.B. K.H.J. was supported by the Carlsberg foundation.

References

Babst BA, Ferrieri RA, Gray DW, Lerdau M, Schlyer DJ, Schueller M, Thorpe MR, Orians CM (2005) Jasmonic acid induces rapid changes in carbon transport and partitioning in *Populus*. New Phytol 167:63–72.

Barbour MM, Hunt JE, Dungan RJ, Turnbull MH, Brailsford GW, Farquhar GD, Whitehead D (2005) Variation in the degree of coupling between $\delta^{13}C$ of phloem sap and ecosystem respiration in two mature *Nothofagus* forests. New Phytol 166:497–512.

Barnard RL, Salmon Y, Kodama N, Sörgel K, Holst J, Rennenberg H, Gessler A, Buchmann N (2007) Evaporative enrichment and time lags between $\delta^{18}O$ of leaf water and organic pools in a pine stand. Plant Cell Environ 30:539–550.

Barthel M, Hammerle A, Sturm P, Baur T, Gentsch L, Knohl A (2011) The diel imprint of leaf metabolism on the $\delta^{13}C$ signal of soil respiration under control and drought conditions. New Phytol 192:925–938.

Behnke HD (1986) Sieve element characters and the systematic position of *Austrobaileya*, Austrobaileyaceae—with comments to the distinction and definition of sieve cells and sieve-tube members. Plant Syst Evol 152:101–121.

Behnke HD (1990) Cycads and gnetophytes. In: Behnke HD, Sjolund RD (eds) Comparative structure, induction and development. Springer, Berlin/Heidelberg/New York, pp 89–101.

Behnke HD, Paliwal GS (1973) Ultrastructure of phloem and its development in *Gnetum gnemon*, with some observations on *Ephedra campylopoda*. Protoplasma 78:305–319.

Bonan GB (2008) Forests and climate change: forcings, feedbacks, and the climate benefits of forests. Science 320:1444–1449.

Bowling DR, McDowell NG, Bond BJ, Law BE, Ehleringer JR (2002) ^{13}C content of ecosystem respiration is linked to precipitation and vapor pressure deficit. Oecologia 131:113–124.

Brandes E, Kodama N, Whittaker K, Weston C, Rennenberg H, Keitel C, Adams MA, Gessler A (2006) Short-term variation in the isotopic composition of organic matter allocated from the leaves to the stem of *Pinus sylvestris*: effects of photosynthetic and postphotosynthetic carbon isotope fractionation. Glob Change Biol 12:1922–1939.

Carbone MS, Czimczik CI, McDuffee KE, Trumbore SE (2007) Allocation and residence time of photosynthetic products in a boreal forest using a low-level ^{14}C pulse-chase labeling technique. Glob Change Biol 13:466–477.

Chang YP (1954) Bark structure of North American conifers. US Department of Agriculture, Washington, DC.

Charnov EL (1976) Optimal foraging, the marginal value theorem. Theor Popul Biol 9:129–136.

Comstedt D (2008) Explaining temporal variations in soil respiration rates and $\delta^{13}C$ in coniferous forest ecosystems. Doctoral thesis, Örebro University, Intellecta DocuSys, Frolunda.

Crafts AS, Crisp CE (1971) Phloem transport in plants. W. Freeman and Company, San Francisco.

Dannoura M, Maillard P, Fresneau C et al. (2011) In situ assessment of the velocity of carbon transfer by tracing ^{13}C in trunk CO_2 efflux after pulse labelling: variations among tree species and seasons. New Phytol 190:181–192.

De Schepper V, Steppe K (2010) Development and verification of a water and sugar transport model using measured stem diameter variations. J Exp Bot 61:2083–2099.

Donghua L, Xinzeng G (1993) Comparative anatomy of the secondary phloem of ten species of Rosaceae. IAWA J 14:289–298.

Ekblad A, Högberg P (2001) Natural abundance of ^{13}C in CO_2 respired from forest soils reveals speed of link between tree photosynthesis and root respiration. Oecologia 127:305–308.

Ekblad A, Boström B, Holm A, Comstedt D (2005) Forest soil respiration rate and $\delta^{13}C$ is regulated by recent above ground weather conditions. Oecologia 143:136–142.

Epron D, Bahn M, Derrien D et al. (2012) Pulse-labelling trees to study carbon allocation dynamics: a review of methods, current knowledge and future prospects. Tree Physiol 32:776–798.

Esau K, Cheadle VI (1958) Wall thickening in sieve elements. Proc Natl Acad Sci USA 44:546–553.

Evert RF, Alfieri FJ (1965) Ontogeny and structure of coniferous sieve cells. Am J Bot 52:1058–1066.

Evert RF, Deshpande BP (1969) Electron microscope investigation of sieve-element ontogeny and structure in *Ulmus americana*. Protoplasma 68:403–432.

Evert RF, Murmanis LM (1965) Ultrastructure of the secondary phloem of *Tilia americana*. Am J Bot 52:95–106.

Hartig T (1837) Vergleichende Untersuchungen über die Organisation des Stammes der einheimischen Waldbäume. J Fort Forstwiss Forstl Naturk 1:125–168.

Högberg P, Högberg MN, Göttlicher SG et al. (2008) High temporal resolution tracing of photosynthate carbon from the tree canopy to forest soil microorganisms. New Phytol 177:220–228.

Hölttä T, Kurppa M, Nikinmaa E (2013) Scaling of xylem and phloem transport capacity and resource usage with tree size. Front Plant Sci 4:496.

Jahnke S, Schlesinger U, Feige GB, Knust EJ (1998) Transport of photoassimilates in young trees of *Fraxinus* and *Sorbus*: measurement of translocation in vivo. Bot Acta 111:307–315.

Jensen KH, Lee J, Bohr T, Bruus H, Holbrook NM, Zwieniecki MA (2011) Optimality of the Münch mechanism for translocation of sugars in plants. J R Soc Interface 8:1155–1165.

Jensen KH, Liesche J, Bohr T, Schulz A (2012*a*) Universality of phloem transport in seed plants. Plant Cell Environ 35:1065–1076.

Jensen KH, Mullendore DL, Holbrook NM, Bohr T, Knoblauch M, Bruus H (2012*b*) Modeling the hydrodynamics of phloem sieve plates. Front Plant Sci 3:151. doi:10.3389/fpls.2012.00151.

Jensen KH, Valente A, Stone HA (2014) Flow rate through microfilters: influence of the pore size distribution, hydrodynamic interactions, wall slip, and inertia. Phys Fluids 26:052004.

Keitel C, Adams MA, Holst T, Matzarakis A, Mayer H, Rennenberg H, Gessler A (2003) Carbon and oxygen isotope composition of organic compounds in the phloem sap provides a short-term measure for stomatal conductance of European beech (*Fagus sylvatica* L.). Plant Cell Environ 26:1157–1168.

Knoblauch M, Peters WS (2010) Münch, morphology, microfluidics—our structural problem with the phloem. Plant Cell Environ 33: 1439–1452.

Kollmann R (1975) Sieve element structure in relation to function. In: Aronoff S, Dainty J, Gorham P, Srivastava L, Swanson C (eds) Phloem transport. Plenum Press, New York, pp 225–242.

Kollmann R, Schumacher W (1963) Über die Feinstruktur des Phloems von *Metasequoia glyptostroboides* und seine Jahreszeitlichen Veränderungen. IV Weitere Beobachtungen zum Feinbau der Plasmabrücken in den Siebzellen. Planta 60:360–389.

Larson PR, Isebrands JG (1974) Anatomy of the primary-secondary transition zone in stems of *Populus deltoides*. Wood Sci Tech 8:11–26.

Lawton JR (1972) Seasonal variations in the secondary phloem of some forest trees from Nigeria. II. Structure of the Phloem. New Phytol 71:335–348.

Leonard OA, Hull RJ (1965) Translocation relationships in and between mistletoes and their hosts. Hilgardia 37:115–153.

Liesche J, Jensen KH, Minchin P, Bohr T, Schulz A (2013) Theoretical and experimental determination of phloem translocation speeds in gymnosperm and angiosperm trees. Acta Hort 991:45–52.

Litton CM, Raich JW, Ryan MG (2007) Carbon allocation in forest ecosystems. Glob Change Biol 13:2089–2109.

MacDaniels LH (1918) The histology of the phloem in certain woody angiosperms. Am J Bot 5:347–378.

McDowell NG, Bowling DR, Bond BJ, Irvine J, Law BE, Anthoni P, Ehleringer JR (2004) Response of the carbon isotopic content of ecosystem, leaf, and soils respiration to meterological and physiological driving factors in a *Pinus ponderosa* ecosystem. Global Biogeochem Cycles 18:1013.

Mencuccini M, Hölttä T (2010) The significance of phloem transport for the speed with which canopy photosynthesis and belowground respiration are linked. New Phytol 185:189–203.

Mildner M, Bader MK-F, Leuzinger S, Siegwolf RTW, Körner C (2014) Long-term ^{13}C labeling provides evidence for temporal and spatial carbon allocation patterns in mature *Picea abies*. Oecologia 175:747–762.

Millburn J, Kallarackal J (1989) Physiological aspects of phloem translocation. In: Baker D, Milburn J (eds) Transport of photoassimilates. John Wiley & Sons, New York, pp 264–305.

Minchin PEH, Lacointe A (2005) New understanding on phloem physiology and possible consequences for modelling long-distance carbon transport. New Phytol 166:771–779.

Moing A, Carde JP (1988) Growth, cambial activity and phloem structure in compatible and incompatible peach/plum grafts. Tree Physiol 4:347–359.

Mortazavi B, Chanton JP, Prater JL, Oishi AC, Oren R, Katul G (2005) Temporal variability in ^{13}C of respired CO_2 in a pine and a hardwood forest subject to similar climatic conditions. Oecologia 142:57–69.

Mullendore DL, Windt CW, Van As H, Knoblauch M (2010) Sieve tube geometry in relation to phloem flow. Plant Cell 22:579–593.

Murmanis L, Evert RF (1966) Some aspects of sieve cell ultrastructure in *Pinus strobus*. Am J Bot 53:1065–1078.

Parthasarathy MV, Tomlinson PB (1967) Anatomical features of metaphloem in stems of *Sabal*, *Cocos* and two other palms. Am J Bot 54:1143–1151.

Peel AJ, Weatherley PE (1962) Studies in sieve-tube exudation through aphid mouth-parts: the effects of light and girdling. Ann Bot 26:633–646.

Petit G, Crivellaro A (2013) Basipetal widening of xylem and phloem conduits along the stem in different woody species. 9th International Workshop on Sap Flow, Ghent.

Plain C, Gerant D, Maillard P, Dannoura M, Dong Y, Zeller B, Priault P, Parent F, Epron D (2009) Tracing of recently assimilated carbon in respiration at high temporal resolution in the field with a tuneable diode laser absorption spectrometer after in situ $^{13}CO_2$ pulse labelling of 20-year-old beech trees. Tree Physiol 29:1433–1445.

Pypker TG, Hauck M, Sulzman EW et al. (2008) Toward using $\delta^{13}C$ of ecosystem respiration to monitor canopy physiology in complex terrain. Oecologia 158:399–410.

Schneider A, Schmitz K (1989) Seasonal course of translocation and distribution of ^{14}C-labelled photoassimilate in young trees of *Larix decidua* Mill. Trees 3:185–191.

Schulz A (1990) Conifers. In: Behnke HD, Sjolund RD (eds) Comparative structure, induction and development. Springer, Berlin/Heidelberg/New York, pp 63–88.

Schulz A (1992) Living sieve cells of conifers as visualized by confocal, laser-scanning fluorescence microscopy. Protoplasma 166:153–164.

Schulz A (1998) Phloem. Structure related to function. Prog Bot 59:429–475.

Schulz A, Behnke HD (1987) Feinbau und Differenzierung des Phloems von Buchen, Fichten und Tannen aus Waldschadengebieten. In: Projekt Europäisches Forschungszentrum für Maßnahmen zur Luftreinhaltung. Kernforschungszentrum Karlsruhe GmbH, Karlsruhe.

Sheehy JE, Mitchell PL, Durand JL, Gastal F, Woodward FI (1995) Calculation of translocation coefficients from phloem anatomy for use in crop models. Ann Bot 76:263–269.

Shibistova O, Yohannes Y, Boy J, Richter A, Wild B, Watzka M, Guggenberger G (2012) Rate of belowground carbon allocation differs with successional habit of two afromontane trees. PLoS One 7:e45540. doi:10.1371/journal.pone.0045540.

Thompson MV, Holbrook NM (2003) Application of a single-solute non-steady-state phloem model to the study of long-distance assimilate transport. J Theor Biol 220:419–455.

Thompson RG, Fensom DS, Anderson RR, Drouin R, Leiper W (1979) Translocation of ^{11}C from Leaves of *Helianthus*, *Heracleum*, *Nymphoides*, *Ipomoea*, *Tropaeolum*, *Zea*, *Fraxinus*, *Ulmus*, *Picea*, and *Pinus*: comparative shapes and some fine structure profiles. Can J Bot 57:845–863.

Turgeon R (2010) The puzzle of phloem pressure. Plant Physiol 154:578–581.

Tyree MT, Christy AL, Ferrier JM (1974) A simpler iterative steady state solution of Münch pressure-flow systems applied to long and short translocation paths. Plant Physiol 54:589–600.

Vogl M (1964) Die Abwanderung von markiertem Phosphor aus dem Pappelblatt. Flora 154:94–98.

Warren JM, Iversen CM, Garten CT Jr et al. (2012) Timing and magnitude of C partitioning through a young loblolly pine (*Pinus taeda* L.) stand using ^{13}C labeling and shade treatments. Tree Physiol 32:799–813.

Watson BT (1980) Effect of cooling on the rate of phloem translocation in the stems of 2 gymnosperms, *Picea sitchensis* and *Abies procera*. Ann Bot 45:219–223.

Weatherley PE, Peel AJ, Hill GP (1959) The physiology of the sieve tube—preliminary experiments using aphid mouth parts. J Exp Bot 10:1–16.

Wheeler JK, Sperry JS, Hacke UG, Hoang N (2005) Inter-vessel pitting and cavitation in woody Rosaceae and other vesselled plants: a basis for a safety versus efficiency trade-off in xylem transport. Plant Cell Environ 28:800–812.

Willenbrink J, Kollmann R (1966) Über den Assimilattransport im Phloem von *Metasequoia*. Z Pflanzenphysiol 55:42–53.

Windt CW, Vergeldt FJ, De Jager PA, Van As H (2006) MRI of long-distance water transport: a comparison of the phloem and xylem flow characteristics and dynamics in poplar, castor bean, tomato and tobacco. Plant Cell Environ 29:1715–1729.

Wooding FBP (1966) The development of the sieve elements of *Pinus pinea*. Planta 69:230–243.

Zimmermann MH (1969) Translocation velocity and specific mass transfer in the sieve tubes of *Fraxinus americana* L. Planta 84:272–278.